Journal of Welding Technology
P-ISSN: 2716-1471 | E-ISSN: 2716-0475
http://e-jurnal.pnl.ac.id/Welding_Technology

Influence of shielding gas flow on the TIG welding process using stainless steel 304 material

Aljufri[1], Sofyan[1], Muhammad Nuzan Rizki[1*], Reza Putra[1], Indra Mawardi[5]
[1]Department of Mechanical Engineering, Universitas Malikussaleh, Lhokseumawe 24355, Indonesia
[2]Department of Mechanical Engineering, Politeknik Negeri Lhokseumawe, Lhokseumawe 24301, Indonesia
[*]Corresponding author: mnuzanrizki@unimal.ac.id

Article Processing Dates:
Received 2024-05-14
Reviewed 2024-06-21
Accepted 2024-06-28
Available online 2023-06-30

Keywords:
Shield Gas Flow
TIG welding
Stainless Steel 304
Mechanical Properties

Abstract

A common issue encountered with main heat exchanger equipment is improper operation, which can lead to the development of cracks in the stainless-steel pipes. The welding process alters the metal microstructure in the heat-affected zone, thereby affecting the mechanical properties of the welded joint. To mitigate this issue, TIG welding with argon shielding gas is employed. This method helps prevent oxidation and ensures the formation of a stable welding arc in 304 stainless steel, which is renowned for its excellent mechanical properties and corrosion resistance. The objective of this study is to evaluate the impact of variations in shielding gas flow on the mechanical properties of 304 stainless steel plates during the TIG welding process. The aim is to determine the optimal settings for producing robust and long-lasting welded joints. To assess the hardness of the welded joints, we employed a Brinell-type Hardness Tester FB-3000LC machine. A Brinell steel ball indenter measuring 5 mm on the HBW scale and applying a load of 125 Kgf was utilized. At a protective gas flow rate of 8 L/min, the average tensile stress was 44.72 N/mm², strain was 0.177, modulus of elasticity was 2518 MPa, and hardness was 99.712 HBW. Increasing the gas flow rate to 13 L/min resulted in an average tensile stress of 47.50 N/mm², strain of 0.189, elastic modulus of 2525 MPa, and hardness of 105.522 HBW. Further increasing the gas flow rate to 18 L/min led to an average tensile stress of 49.69 N/mm², strain of 0.192, modulus of elasticity of 2597 MPa, and hardness of 106.704 HBW. Based on the research findings, it was observed that the weld area exhibited an increase in hardness values due to the heat generated during the welding process. The use of protective gas flow during welding is deemed effective in producing well-formed welded joints, as it prevents fractures from occurring within the weld area during the tensile test process. The choice of protective gas is determined by the dimensions of the material plate.

1. Introduction

In the industrial world, which is experiencing very modern developments such as today, the welding connection process makes a major contribution to manufacturing construction. The application of welded joints in manufacturing is very massive, such as in ship construction, building construction, the railway industry, and others [1-5]. Welding seems simple, but there are many problems that must be overcome, the solution of which requires various approaches. For this reason, welding is very important and requires serious handling in its application [6-7].

Damage often occurs in machine-constructed welded joints, one of the cases that often occurs is in MHE (main heat exchanger) generating equipment. During operation, the MHE is always observed, and all its parameters are studied. Changes in pressure and changes in the methane element in the MCR (Multi-Component Refrigerant) will indicate that the MHE has been damaged and needs to be repaired. This damage can occur due to the influence of operating conditions such as cracks and leaks in the pipe. The connecting pipe on the outside of the MHE was made of stainless steel [8].

The metal will experience the effects of heating due to welding and changes in the microstructure around the weld area [9].The weld metal and the heat-affected zone (HAZ), where if the protective gas does not properly protect the weld metal, it affects the microstructure of the weld area because it gets hotter during the welding process, then the welding area, or what is known as the HAZ area, will create a recrystallization effect, namely causing grains to form in the area [10-11]. The HAZ increases with weld defects such as porosity. If these grains become larger, the mechanical properties of the weld change [12].

Tungsten arc welding (TIG) is welding using an arc flame, which produces a fixed electrode made of tungsten, while the additional material is made of the same material as the material being welded and is separate from the torch. To prevent oxidation, a protective gas was used. of the torch in the form of Ar gas [13]. Protective gas is a component of the welding process that protects the welding process of the weld metal and weld pool from contamination by the surrounding air, which results in an imperfect mixture between the added material (filler rod) and the liquid material being joined [14]. Argon has a low ionization potential; therefore, the resulting welding arc is stable and has little spatter.

Stainless steel is a high-alloy steel material with rust-resistant properties. This steel contained a minimum of 10.5% Cr. Some stainless steels containing more than 30% Cr or less than 50% Fe are known as special stainless steels, for example, AISI 440C, ASTM A240, and ASTM A268 [15], [16-17]. Stainless steel 304 is the most commonly used metal because it has the best combination of mechanical properties and corrosion resistance [18-19]. It is widely used in industry, and on a small scale, its uses include tanks and containers [20]. Low carbon content can increase resistance to grain boundary corrosion (intergranular corrosion), and the low carbon content of Stainless Steel 304 of 0.03 wt% causes little carbide precipitation to form [21].

This research aims to determine the effect on the weld area due to the process of varying the protective gas flow carried out using Tungsten Inert Gas (TIG) welding on the mechanical properties of a stainless steel 304 plate to determine whether the use of the protective gas flow used in this research can produce joints. good weld.

Welding is the process of joining two or more metal parts using heat energy. Based on the definition of the American Welding Society (AWS), welding is a metallurgical bond in a metal or metal alloy joint that is carried out in a melted or liquid state. Welding, according to DIN (Deutsche Industry Norman), is a metallurgical bond in a metal or metal alloy joint that is carried out in a melted or liquid state [22].

Electrodes are often called additives, electrodes are usually grounded at an angle of 60° to 90° for manual welding. For mechanical applications, the tip angle determines the shape of the arc and influences the weld pool penetration profile. The consistency in the grinding tip must be noted, and the condition between the welds must be checked.

In a welded joint, the tensile properties and hardness of the material are strongly influenced by the properties of the base metal. The properties of the weld metal and the dynamic properties of the joint are closely related to geometry and stress. The test carried out is a tensile strength test because, apart from observing the similarities between the parent metal in the welding area, it also determines the characteristics of the material to be tested during bending and machining.

Equation (1) to (3) are used to calculate tensile properties:

$$\sigma = \frac{P}{Ao} \tag{1}$$

And

$$e = \frac{(Li-Lo)}{Lo} \times 100\% \tag{2}$$

$$E = \frac{\sigma}{\varepsilon} \tag{3}$$

The Brinell Hardness value can be calculated using the following Equation (4):

$$HBS = \frac{2Fkgf}{(\pi D\left(D-\sqrt{D^2-d^2}\right))} \tag{4}$$

2. Research Methods

The material used in this research is stainless steel 304 with a test dimensions of 200x20x5 mm, as shown in Fig. 1. SS 304 stainless steel is an alloy steel with a composition of 0.042% C, 1.19% Mn, 0.034% P, 0.006% S, 0.049% Si, 18.24% Cr, 8.15% Ni, and the remaining Fe [23]. with a Yield Strength of 205 MPa, Tensile Strength of 515 MPa, Elongation of 40%, and hardness 201 HRB [24].

Welding was performed using an Argon TID DC IGBT Inverse T 350 H welding machine. The electrodes used were tungsten and helium, which use a current strength of 110 A. After undergoing the TIG welding process with a V-seam angle of 40°, the specimens were formed according to ASTM E8 standards for tensile testing. The number of test objects was 15, divided into 3 groups of variations in the flow rate of the protection gas, namely 8, 13, and 18 liters per minute.

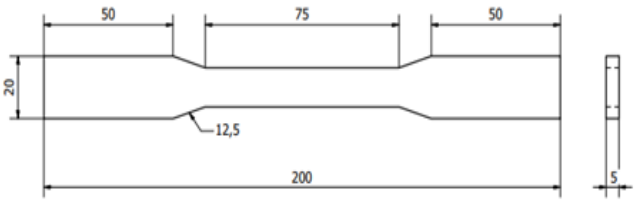

Fig. 1. Tensile Test Specific Dimensions.

The research flow diagram for this research is shown in Fig. 2.

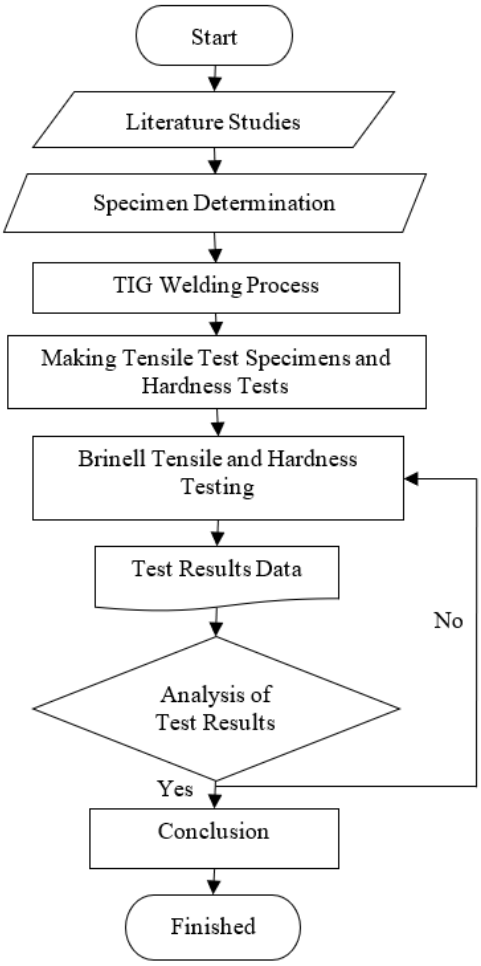

Fig. 2. The stages of the research are generally described using a flow diagram.

The same material was formed according to the ASTM E10 standard to form a Brinell hardness test specimen, as shown in Fig. 3. The number of test specimens was 3 for each variation of protective gas flow rate of 8 liters/minute, 13 liters/minute, and 18 liters/minute.

By making V-groove angles with a slope of 40° using a milling machine, cutting was performed by hand grinding for a total of 18 specimens. The welding process with variations in protective gas flow of 8 liters/minute, 13 liters/minute, and 18 liters/minute was carried out at the Lhokseumawe State Polytechnic Laboratory, tensile testing at the Lhokseumawe State Polytechnic Laboratory, and Brinell hardness testing at the Medan State Polytechnic Mechanical Engineering Laboratory. The protective gas flow rate used in this research was 8 liters/minute, 13 liters/minute, and 18 liters/minute.

Pure argon was used as the protective gas. This welding specimen uses variations in the flow rate of the shielding gas, which is shown in Fig. 4.

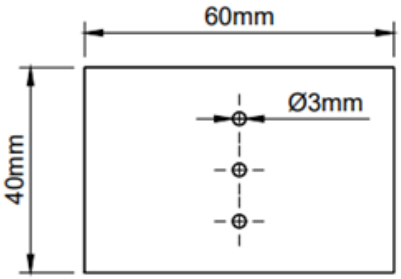

Fig. 3. Dimensions of ASTM E10 Brinell hardness test specimen.

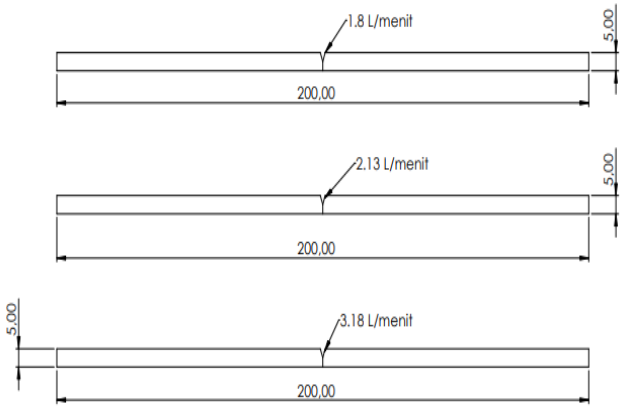

Fig. 4. Research Specimen.

Tensile testing and hardness testing were carried out with the aim of determining the mechanical properties of Stainless Steel 304 from TIG welding with variations in shielding gas flow and V seam angle with a slope of 40°. Tensile testing was performed using a Computer Hydrolic Testing Machine Type HT-9502, and Brinell hardness testing was performed using a Brinell Hardness Tester LC-3000LC. In the hardness test, the area tested was the welding area.

In this research, there are independent variables and fixed variables. The independent variable in this research is the variation in protective gas flow discharge. Meanwhile, the fixed variable that will be used is TIG welding using a single V seam, stainless steel 304 material, with tensile tests on the results of the welded joints.

3. Results and Discussion.

The results of the analysis of the influence of variations in the flow of shielding gas used in the TIG welding process on the tensile strength and material hardness of 304 stainless steel plates are explained in several explanatory points below. In the welding process, for all variations of the shielding gas flow, the welding results were obtained, as shown in Fig. 5.

Specimens that have been TIG welded on stainless steel 304 material using E308L electrodes and have been formed according to ASTM E8 standards are then subjected to a tensile testing process [25]. After testing, the fracture that occurred as a result of the tensile test was in the part with the lowest strength compared to other parts, namely the base metal. This indicates that the strength of the welded part is stronger than that of the base metal part, so that the fracture occurs due to the distribution of heat to the base metal area which is caused by penetration during the welding process and due to the tensile force being too large when the tensile test is carried out. An image of the fracture in the base metal area is shown in Fig. 6

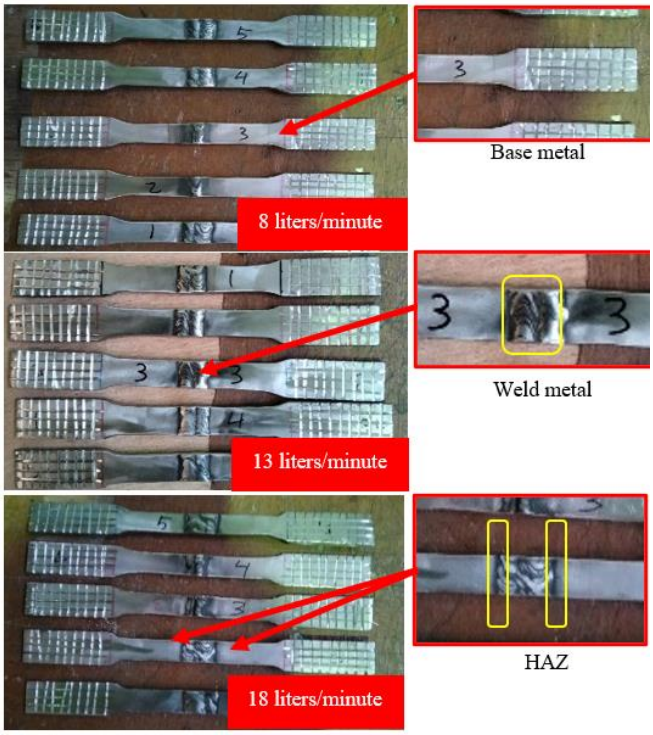

Fig. 5. Welding results for three variations in shielding gas flow.

Fig. 6. Fracture results that occurred during the tensile test process for specimens with a protective gas flow of 8 L/min.

The data obtained after the tensile test at a protective gas flow of 8 liters/minute were, firstly, the final length increase that occurred in specimen one was 230 mm, specimen two was 238 mm, specimen three was 235 mm, specimen four was 240 mm and specimen five was 234 mm. The maximum loads obtained for specimen one were 3865, 4479, 4626, 4487, and 4462 kg, respectively.

Furthermore, an image of the specimen after the tensile test process at a protective gas flow of 13 liters per minute is shown in Fig. 7 below.

The data obtained after the tensile test at a protective gas flow of 13 liters/minute were, firstly, the final increase in length occurred in specimen one with a value of 242 mm, specimen two was 239 mm, specimen three was 236 mm, specimen four was 233 mm and specimen five was 239 mm. mmm. Then the maximum load obtained on specimen one is 4836 Kgf, specimen two 4736 Kgf, specimen three 4504 Kgf, specimen four 4570 Kgf, and specimen five 4632 Kgf.

Fig. 7. Fracture after tensile test at a protective gas flow of 13 L/min.

Then a picture of the specimen after the tensile test process was carried out at a protective gas flow of 18 liters per minute is shown in Fig. 8.

Fig. 8. Fracture after tensile test at a protective gas flow of 18 L/min.

The data obtained after the tensile test at a protective gas flow of 18 liters/minute were, firstly, the final length increase that occurred in specimen one was 239 mm, specimen two was 240 mm, specimen three was 239 mm, specimen four was 241 mm and specimen five was 233 mm. . Then the maximum load obtained on specimen one is 4915 Kgf, specimen two is 4954 Kgf, specimen three is 4881 Kgf, specimen four is 4991 Kgf, and specimen five is 4612 Kgf.

From the data mentioned above, after that, calculations were carried out for the values of tensile stress, strain, and modulus of elasticity at a protective gas flow of 8 liters per minute, and the results obtained is shown in Table 1.

Table 1. Results of tensile test calculations at a protective gas flow of 8 L/min.

No Specimen	Tensile Stress (N/mm²)	Strain (%)	Modulus of Elasticity (MPa)
1	39,43	0,15	2628
2	45,70	0,19	2405
3	47,20	0,175	2697
4	45,78	0,20	2289
5	45,53	0,17	2572
Average	44,728	0,177	2518,2

The values of tensile stress, strain, and modulus of elasticity at a protective gas flow of 13 liters per minute, the results obtained is shown in Table 2.

Table 2. Results of tensile test calculations at a protective gas flow of 13 L/min.

No Specimen	Tensile Stress (N/mm²)	Strain (%)	Modulus of Elasticity (MPa)
1	49,34	0,21	2349
2	48,32	0,195	2477
3	45,96	0,18	2553
4	46,63	0,165	2826
5	47,26	0,195	2423
Average	47,502	0,189	2525,6

The tensile stress, strain, and modulus of elasticity values at a protective gas flow of 18 liters/minute and the results obtained is shown in Table 3.

Table 3. Results of tensile test calculations at a protective gas flow of 18 L/min.

No Specimen	Tensile Stress (N/mm²)	Strain (%)	Modulus of Elasticity (MPa)
1	50,15	0,195	2571
2	50,55	0,20	2527
3	49,80	0,195	2553
4	50,93	0,205	2484
5	47,06	0,165	2852
Average	49,698	0,192	2597,4

- Tensile test results

The data from the calculation of tensile stress, strain, and modulus of elasticity above is compared to determine the differences that occur in variations in protective gas flow of 8 liters per minute, 13 liters per minute, and 18 liters per minute.

From Fig. 9 (a), we can see that the tensile stress value that occurs at a variation of 8 L/min experiences an increasing trend. while for variations 13 and 18 L/min, there is a decreasing trend. The comparison graph for tensile stress is shown in Fig. 9 (b).

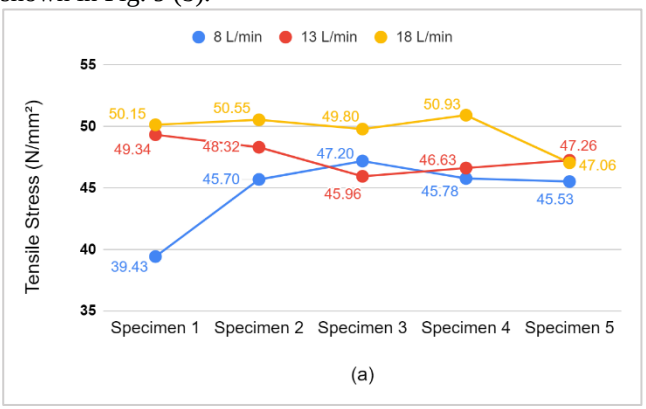

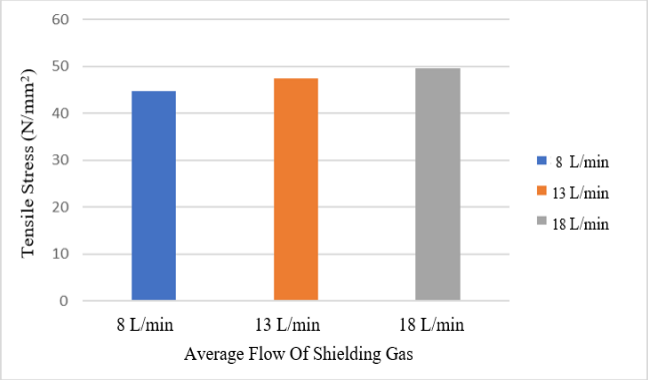

(b)

Fig. 9. (a) Comparison of the tensile stress value with variations in shielding gas flow, (b) Comparison of tensile stress values in the shielding gas flow.

Fig. 9 (b) show the test results show that between the five specimens with variations in protective gas flow, the tensile stress value obtained from the specimens with variations in protective gas flow was 8 liters/minute with an average value of 44.72 N/mm2, while the tensile stress value of the specimen obtained by varying the protective gas flow was 13 liters/minute with an average value of 47.50 N/mm2, and the tensile stress value of the specimen was obtained by varying the protective gas flow of 18 liters/minute with an average value of 49.69 N/mm2.

The three variations in protective gas flow, the highest tensile stress value is found in the welded specimen using a protective gas flow of 18 liters/minute with an average value of 49.69 N/mm^2. This value is slightly different from other protective gas flow variations, while the lowest tensile stress value is found in the welded specimen using a protective gas flow variation of 8 liters/minute with an average value of 44.72 N/mm2. . From the graphic image of the tensile test results above, it shows that the tensile test results vary. This explains that the weld area has good and poor strength, as evidenced by the fact that fractures do not occur in the weld. This shows optimal strength where the use of variations in the flow of protective gas has a significant effect. Good.

- Calculation results for strain values

The strain comparison graph for variations in protective gas flow, to see the increase in length of an object that has been subjected to a force during the test, is shown in Fig. 10.

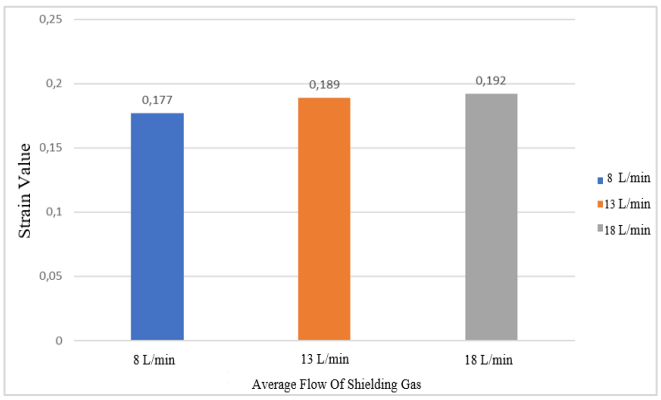

Fig. 10. Comparison of tensile strain values with protective gas flow.

Fig. 10 shows the five welded specimens that have varying strain values. The welded specimen using a protective gas flow of 8 L/min obtained an average value of 0.177, while the welded specimen using a protective gas flow of 13 L/min obtained an average value of 0.189, and the welded specimen using a shielding gas flow of 18 L/min obtained an average value of 0.192.

Fig. 10 shows that the highest and lowest values obtained by the welded specimen using a protective gas flow of 18 liters/minute have the highest value with an average strain value of 0.192; this value is different from other protective gas flow values, while the lowest strain value is found in the specimen. welding using a protective gas flow of 8 liters per minute with an average value of 0.177.

- Calculation results for the elastic modulus value

A comparison graph of the modulus of elasticity for variations in protective gas flow is shown in Fig. 11.

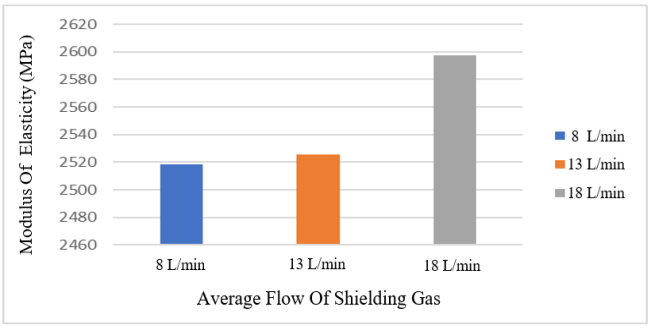

Fig. 11. Comparison of elastic modulus values for shielding gas flow

Fig. 11. show that among the five welded specimens that underwent testing, the elastic modulus values varied. This is shown in the welded specimens that used a protective gas flow of 8 liters/minute with an average value of 2518 MPa, while the elastic modulus value used variations in protective gas flow. 13 liters per minute has an average value of 2525 MPa, while welded specimens using a shielding gas flow of 18 liters per minute get an average value of 2597 MPa. It can be explained from the graph above that the highest average value of elastic modulus uses a protective gas flow of 18 liters/minute with an average value of 2597 MPa, while the lowest average value of elastic modulus is found in specimens using a protective gas flow of 8 liters/minute with an average value of 2518 MPa. From the graphic image of the modulus of elasticity results above, it shows the varying tensile test results, which explains the large influence on the use of protective gas flow and the weld seam used.

- Hardness test results

Specimens that have been TIG welded on stainless steel 304 material using electrodes and welding wire and have been established to the ASTM E10 standard for the Brinell hardness testing process are then carried out.

In this Brinell test, the HBW scale was used with a steel ball indenter with a diameter of 5 mm and a test load of 125 KgF [26]. Tests were carried out in the welding area. An image of the Brinell hardness test specimen is shown in Fig. 12. The Brinell hardness test results are listed in Table 4.

Fig. 12. Hardness Test Specimen.

Table 4. Brinell Hardness Test Data.

Test Number	Shield Gas Flow		
	8 liters/minute	13 liters/minute	18 liters/minute
1	97,890	108,730	101,610
2	101,278	103,635	108,048
3	99,967	104,150	110,454
Average	99,712	105,522	106,704

After testing the Brinell hardness, the hardness values in the protective gas flow of 8 liters/minute, 13 liters/minute, and 18 liters/minute is shown in the comparison of what occurs in the protective gas flow in Fig. 13 below:

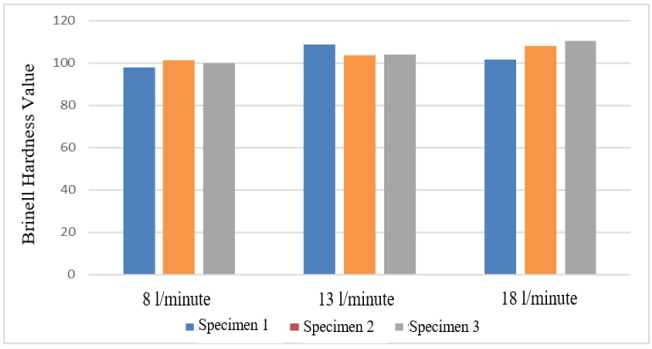

Fig. 13. Comparison of hardness values in the shielding gas flow.

Brinell hardness in Fig. 4.11 above show that a protective gas flow of 8 liters/minute with a value for specimen one = 97,890 HBW, specimen two = 101,278 HBW, and specimen three = 99,967 HBW. Brinell hardness value with a protective gas flow of 13 liters/minute with a value for specimen one = 108,780 HBW, specimen two = 103,635 HBW, and specimen three = 104,150 HBW. At a protective gas flow of 18 liters per minute, the Brinell hardness value obtained for specimen one was 101,610 HBW, specimen two was 108,048 HBW, and specimen three was 110,454 HBW. The comparison data for hardness testing on variations in protective gas flow rate is shown in Fig. 14.

From the research results, it was found that the average value of the protective gas flow variation of 8 liters per minute resulted in an average hardness value of 99.712 HBW, the protective gas flow variation of 13 liters per minute had an average hardness value of 105.522 HBW, and the protective gas flow variation of 18 liters per minute had an average value of 106,704 HBW. The largest average hardness value was at a protective gas flow of 18 L/minute with a value of 106,704 HBW, while the lowest average value was produced at a protective gas flow variation of 8 liters/minute with a value of 99,712 HBW.

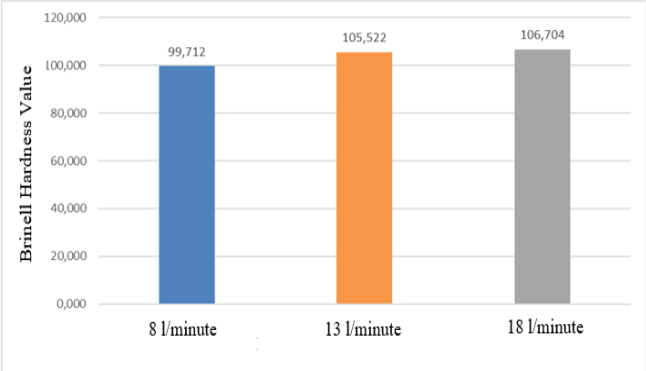

Fig. 14. Comparison of Brinell hardness values with variations in shielding gas flow.

From the data displayed in the Fig. above, it can show that the effect of variations in the shielding gas flow on the hardness is directly proportional; that is, the greater the shielding gas flow, the greater the hardness of the resulting weld. The greater the value of the protective gas flow, the greater the amount of the pearlite structure. This is because the greater the flow of protective gas, the stronger the pressure of the protective gas blowing, the faster the cooling rate, and the greater the release of protective gas, which increases the level of hardness in the welded joint.

Shielding gas can influence the transfer of filler metal from the arc to the weld joint, which contributes to the efficiency of the welding process and weld quality by determining the weld penetration profile, thus greatly influencing the strength of the material, especially between the HAZ area and the base metal (SS304).

4. Conclusions.

The lowest ultimate tensile strength (UTS) value was recorded at a gas flow of 8 L/min with a value of 2518 MPa, while the highest value occurred at a gas flow of 18 L/min with a value of 2597 MPa. This difference is caused by variations in gas flow during the welding process. The effect of the shielding gas flow on the hardness shows a unidirectional relationship; that is, the greater the shielding gas flow, the higher the resulting weld hardness. This is because increasing the shielding gas flow increases the amount of the pearlite structure. A larger shielding gas flow results in a stronger gas pressure, faster cooling rates, and greater gas release, all of which contribute to the increased hardness of the weld joint. Shielding gas also influences the transfer of the filler metal from the arc to the weld joint, which influences the efficiency of the welding process and the quality of the weld by determining the weld penetration profile. This significantly affects the strength of the material, particularly between the HAZ area and the base metal (SS304). The greater the shielding gas flow, the higher the hardness value of the weld material, with the largest increase in hardness occurring in the weld area because the metal in this area melts with the electrode and experiences a faster cooling rate.

References.

[1] A. A. Tohari, "Pengaruh Kecepatan Aliran Gas Pelindung Las MIG Baja SS-540." JTM Unesa, vol. 9, no. 1, 2021, Available: https://ejournal.unesa.ac.id/index.php/jtm-unesa/article/view/38246

[2] E. Karayel and Y. Bozkurt, "Additive manufacturing method and different welding applications," *Journal of Materials Research and Technology*, vol. 9, no. 5, pp. 11424–11438, Sep. 2020, doi: 10.1016/j.jmrt.2020.08.039.

[3] Y. M. Zhang, Y.-P. Yang, W. Zhang, and S.-J. Na, "Advanced Welding Manufacturing: A Brief Analysis and Review of Challenges and Solutions," *J Manuf Sci Eng*, vol. 142, no. 11, Nov. 2020, doi: 10.1115/1.4047947.

[4] J. Zhao *et al.*, "Dynamic constitutive model of U75VG rail flash-butt welded joint and its application in wheel-rail transient rolling contact simulation," *Eng Fail Anal*, vol. 134, p. 106078, Apr. 2022, doi: 10.1016/j.engfailanal.2022.106078.

[5] A. Królicka, K. Radwański, R. Kuziak, T. Zygmunt, and A. Ambroziak, "Microstructure-based approach to the evaluation of welded joints of bainitic rails designed for high-speed railways," *J Constr Steel Res*, vol. 175, p. 106372, Dec. 2020, doi: 10.1016/j.jcsr.2020.106372.

[6] B. Wang, S. J. Hu, L. Sun, and T. Freiheit, "Intelligent welding system technologies: State-of-the-art review and perspectives," *J Manuf Syst*, vol. 56, pp. 373–391, Jul. 2020, doi: 10.1016/J.JMSY.2020.06.020.

[7] A. B. Pereira and F. J. M. Q. de Melo, "Quality Assessment and Process Management of Welded Joints in Metal Construction—A Review," *Metals (Basel)*, vol. 10, no. 1, p. 115, Jan. 2020, doi: 10.3390/met10010115.

[8] H. Sunandrio *et al.*, "Analisis Kerusakan Tube Thermocouple Pada Reaktor Hydrocracking Di Kilang Pengolahan Minyak Bumi."

[9] F. Habibi, S. Mulyo, and B. Respati, *Perlakuan Pemanasan Awal Elektroda Terhadap Sifat Mekanik Dan Fisik Pada Daerah Haz Hasil Pengelasan Baja Karbon St 41*. SNST 6 (2015).

[10] S. K. Sharma, S. Maheshwari, and R. K. R. Singh, "Modeling and Optimization of HAZ Characteristics for Submerged Arc Welded High Strength Pipeline Steel," *Transactions of the Indian Institute of Metals*, vol. 72, no. 2, pp. 439–454, Feb. 2019, doi: 10.1007/s12666-018-1495-5.

[11] A. Jain, B. Singh, and Y. Shrivastava, "Analysis of heat affected zone (HAZ) during micro-drilling of a new hybrid composite," *Proc Inst Mech Eng C J Mech Eng Sci*, vol. 234, no. 2, pp. 620–634, Jan. 2020, doi: 10.1177/0954406219877911.

[12] S. Junus, "Pengaruh Besar Aliran Gas terhadap Cacat Porositas dan Struktur Mikro Hasil Pengelasan MIG pada Paduan Aluminium 5083," *ROTOR*, vol. 4, no. 1, pp. 22–30, Jan. 2011.

[13] I. Apriadi, J. waluyo, A. Duniawan, P. S. Studi Teknik Mesin, and J. Teknik Mesin, "Pengaruh kecepatan Pengelasan Tungsten Inert Gas Terhadap Sifat Fisis dan mekanis Pada Pengelasan Baja Karbon Menengah." *SIMETRIS (2020) 14(1) 16-17.*

[14] Z. Hilmy, N. Syahroni, and Y. S. Hadiwidodo, "Analisa Pengaruh Variasi Komposisi Gas Pelindung Terhadap Hasil Pengelasan Gmaw-Short Circuit dengan Penggunaan Mesin Khusus Regulated Metal Deposition (RMD)," pp. 219–226, 2018.

[15] L. Pan, C. T. Kwok, and K. H. Lo, "Friction-stir processing of AISI 440C high-carbon martensitic stainless steel for improving hardness and corrosion resistance," *J Mater Process Technol*, vol. 277, p. 116448, Mar. 2020, doi: 10.1016/j.jmatprotec.2019.116448.

[16] Z. Tan, R. Xu, H. Bi, Z. Zhang, and M. Li, "Effects of potential on corrosion behavior and contact resistance of 446 stainless steel in simulated proton exchange membrane fuel cell cathode environment," *Journal of Solid State Electrochemistry*, vol. 27, no. 8, pp. 1993–2003, Aug. 2023, doi: 10.1007/s10008-023-05469-y.

[17] R. G. Tayactac and E. B. O. Ang, "A Review of Corrosion Resistance Alloy Weld Overlay Cladding Material for Geothermal Applications," *Materials Science Forum*, vol. 1047, pp. 120–127, Oct. 2021, doi: 10.4028/www.scientific.net/MSF.1047.120.

[18] A. Kumar, R. Sharma, S. Kumar, and P. Verma, "A review on machining performance of AISI 304 steel," *Mater Today Proc*, vol. 56, pp. 2945–2951, Jan. 2022, doi: 10.1016/J.MATPR.2021.11.003.

[19] G. S. Was and S. Ukai, "Austenitic Stainless Steels," in *Structural Alloys for Nuclear Energy Applications*, Elsevier, 2019, pp. 293–347. doi: 10.1016/B978-0-12-397046-6.00008-3.

[20] Sumarji, "Studi Perbandingan Ketahanan Korosi Stainless Steel Tipe Ss 304 Dan Ss 201 Menggunakan Metode U-Bend Test Secara Siklik Dengan Variasi Suhu Dan Ph," *ROTOR*, vol. 4, no. 1, pp. 1–8, 2011.

[21] V. Ayu, S. Institut, T. Adhi, T. Surabaya, and E. Widodo, *Analisis Kekuatan Tarik dan Karakteristik XRD pada Material Stainless Steel dengan Kadar Karbon yang Berbeda*. 2017. [Online]. Available: https://www.researchgate.net/publication/324434551

[22] Aditia, Nurdin, and A. S. Ismy, "Analisa Kekuatan Sambungan Material AISI 1050 dengan ASTM A36 dengan Variasi Arus pada Proses Pengelasan SMAW," *Journal of Welding Technology*, vol. 1, no. 1, pp. 1–4, 2019.

[23] I. Saputra, "Micro structure analysis of 304 stainless steel in the TC-ISSF installation," in *2018*, Proceedings of the Research Presentation and Activities of the Radioactive Waste Technology Center, 2019, pp. 1–34. Accessed: Jun. 24, 2024. [Online]. Available: https://inis.iaea.org/search/search.aspx?orig_q=RN:51070203

[24] V. A. Setyowati, D. E. Wahyu, R. Widodo, and T. Surabaya, "Analisis Kekuatan Tarik Dan Karakteristik Xrd Pada Material Stainless Steel Dengan Kadar

Karbon Yang Berbeda," *Seminar Nasional Sains dan Teknologi Terapan V* , pp. 57–62, 2017.

[25] ASTM Internasional, "Designation: E8/E8M − 13a Standard Test Methods for Tension Testing of Metallic Materials 1," 2013. doi: 10.1520/E0008_E0008M-13A.

[26] P. Organek, B. Gosowski, and M. Redecki, "Relationship between Brinell hardness and the strength of structural steels," *Structures*, vol. 59, p. 105701, Jan. 2024, doi: 10.1016/j.istruc.2023.105701.